

# Design of a Semiautonomous Biomimetic Underwater Vehicle for Environmental Monitoring.

Madis Listak  
Institute of Computer Engineering  
Tallinn University of Technology  
Ehitajate tee 5, 19086 Tallinn  
ESTONIA  
*Madis.Listak@mail.ee*

Georg Martin  
Estonian Marine Institute,  
10617, Tallinn,  
ESTONIA  
*georg@klab.envir.ee*

Deivid Pugal, Alvo Aabloo, Maarja Kruusmaa  
Institute of Technology  
University of Tartu  
Vanemuise 21, 51014 Tartu  
ESTONIA  
*Maarja.Kruusmaa@ut.ee*

**Abstract** – This paper describes a preliminary prototype of a fishlike biomimetic underwater robot. The goal is to develop a semiautonomous vehicle for environmental monitoring in shallow waters. We describe the vehicle and discuss the environmental factors that have influenced the design. Experimental results illustrate the performance of the prototype.

This paper describes task requirements and the design of the prototype. We also represent some experimental results from this early stage of the prototype development and some characteristics of its performance. We finish this paper with conclusions and remarks about the future work directions.

## I. INTRODUCTION

Biomimetic underwater vehicle design has attracted the attention of researchers for several reasons. Fishes and other aquatic animals are efficient swimmers. They have remarkable manoeuvrability, trajectory following capability and they efficiently stabilize themselves in currents and surges. They also leave a less noticeable wake than conventional underwater vehicles equipped with thrusters. Artificial aquatic creatures also help us to understand how their biological counterparts are functioning.

Biomimetic underwater devices reported so far include a robotic tuna fish [1, 2], buoyancy control inspired by sperm whales [3], control of a fish by means of caudal fin [4] or pectoral fins [5]. In [6] an exhibition system is proposed for enhancing event spaces that includes an animatronics system for modern-day fish, coelacanth, and Cambrian world creatures, able to swim under their own electric power. Most of the biomimetic underwater vehicles mimic carangiform swimming (propulsion through the water with oscillating movements of the tail and the rear part of the body) [7]. Other types of swimming are also implemented like for example anguilliform (eel-like) locomotion [8] and locomotion with help of elongated pectoral fins [9, 10].

Most of this research is carried out mainly because of scientific purposes with the motivation to investigate and implement mechanics and kinematics of swimming and to develop new control algorithms for fish-like locomotion.

In the opposite to the above cited studies the design of the robot described in this paper is motivated by the task requirements. The main goal of development of this device is environmental monitoring in shallow waters of the coastal regions in Baltic Sea and in inland surface water bodies. The biomimetic design of the vehicle is the most suitable one for the task requirements. The main objective of this study is not to implement any certain type of mechanical design, swimming mode or control method but to build a device for practical use for environmental scientists. In the first hand it is meant for doing the laborious, expensive and dangerous work that is at present done by divers.

### A. Design considerations

Baltic Sea is a closed and shallow sea. The depth of Baltic Sea is down to 80m but the regions most interesting for environmental inspection usually lie near the coastline at the depth down to 20m. On the eastern and southern coast of the sea shallow bays are often only few meters deep.

Most of the research and product development of underwater vehicles is directed towards exploitation in much deeper water [11]. Commercial vehicles are used mainly by offshore oil and gas industry for exploitation and exploration of oil and gas fields or for scientific deep ocean surveys. Also military vehicles basically used for reconnaissance, intelligence gathering and demining are capable of operating in much deeper water.

These vehicles are usually heavy, they tolerate high pressure and they are very expensive. Vehicles for shallow water on the contrary do not have to be especially strong and powerful that makes their building and using easier and cheaper.

At the same time vehicles operating in a very shallow water and surf zone face different kind of design problems [12]. Their weight and size has to be kept small, they require good manoeuvrability, which is especially difficult to achieve in surges. An important part of environmental inspection is the regular monitoring of macro vegetation and therefore the most difficult regions are the most interesting for environmental scientists. In shallow bays some algae can grow up to 1m – 1.5m and reach up to the water surface. A vehicle operating in such an environment has to be able to move in dense vegetation.

Since the coasts of Baltic Sea are densely inhabited, fishing nets, harbours, surface transportation and beaches make the environmental conditions even more complicated.

Different from tropical or subtropical seas and deep ocean, water in Baltic Sea is very turbid. During summer, when water contains lots of zoo- and phytoplankton, visibility is often only few meters or even less in a surf zone.

Seabed of Baltic Sea is to a great extent covered with mud or extremely volatile detritus, mainly particles of zoo and phytoplankton that has settled down.

Conventional underwater vehicles almost unexceptionally propel themselves through the water with the help of thrusters [13]. The advantages of thrusters are that they are powerful, efficient, able to move the vehicle with a high speed and are commercially available. Also there exist advanced methods to control underwater vehicles with thrusters [14].

The disadvantage of thrusters is that they create strong turbulence. This feature makes it difficult to design a vehicle with thrusters that meet the requirements of the task description. On the one hand visibility is very low. Therefore a vehicle that is used for benthic surveys, like monitoring underwater vegetation or bottom morphology, has to be close to the seabed. On the other hand, if the vehicle creates turbulence close to the seabed, visibility becomes practically zero and monitoring of the bottom is not possible.

Current AUV-s and ROV-s are also mostly operated from ships and weight often hundreds of kilos or tons. This is impossible in Baltic Sea, no ship can enter the zones interesting for biologist. Therefore our device must be light enough to operate from an inflatable boat.

## II. DESIGN CONCEPT

### A. Semiautonomous and remotely operated modes

Since different types of missions require different performance, the vehicle is designed to be used in two different modes.

1) *Towing mode*. In this mode the vehicle is towed behind a boat. This mode is used for repetitive surveys of the seabed. The main challenge is to keep a constant distance from bottom and not to collide with the boulders and rocks that are common in the sea.

2) *Remote control mode*. In this mode the robot must stabilize itself over certain points of interest. That means manoeuvring backward and forward and also stabilizing in currents. This mode can be used for close inspection, taking water samples or diving under ice.

### B. Horizontally and vertically compressed modes

The shell of the robot has a flattened ellipsoidal shape. Depending on the task of the robot, the vehicle can be used in two different orientations (Fig. 1).

1) *Horizontally compressed*. This orientation will be mostly used at towing mode. The advantage of the horizontally compressed shape is that the whole body of the vehicle operates as an elevator and works against lift forces. Horizontally flattened body can also be used to submerge to the seabed for a closer inspection. Since its cross section is smaller than of the vertically compressed body, it is easier to stabilize the vehicle in lateral currents.

1) *Vertically compressed*. This orientation will be mostly used in a remote controlled mode and in a towing mode at low speeds in very shallow waters with opulent vegetation. A laterally compressed vehicle is able to heave and submerge faster at low speeds and has better manoeuvrability

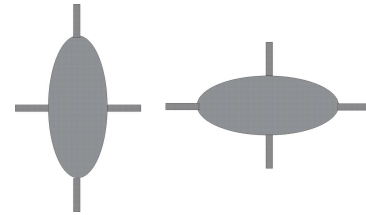


Fig. 1. Orientation of the vehicle: vertically compressed (to the left) and horizontally compressed (to the right).

## III. MECHANICAL STRUCTURE

The layout of the interior of the vehicle is represented in Fig. 2. Since our aim is to keep the cost of the vehicle low, the prototype is built from off-the-shelf components that are easily replaceable.

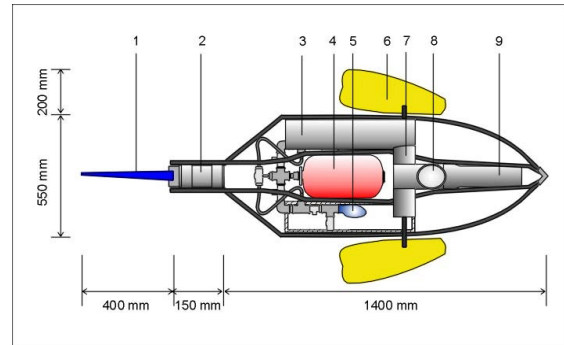


Fig. 2. Internal layout of the vehicle (1-fin, 2-stepper, 3-PVC tube, 4-compressed air tank, 5-rubber tank, 6-fin, 7-stepper, 8-camera, 9-batteries and electronics)

The streamlined hull of the vehicle houses the pneumatic system, servos and stepper motors to control the control surfaces, electronic circuits, batteries and sensors. The supporting rod of the vehicle is used to fix these components. The hull is floodable and made of fibreglass. Openings in the hull are for cameras, forward and bottom-looking sonar, lights, and to attach the rudders to the body of the vehicle.

Variable ballast tanks are placed at both sides of the vehicle and made of PVC tubes. Trimming weights can be added or removed from the bow and stern ends of these tubes to compensate changes in buoyancy when modules are changed or payload is added.

The compressed air balloon is fixed between the supporting rods between the ballast tanks at the centre of the vehicle.

The PVC tube in the bow part of the vehicle is a watertight compartment sealed with a silicon sealant and fixed between the supporting skeletons. This compartment houses control electronics and batteries for emergency cases. When the off-board power supply is disconnected or communication with the surface control unit is lost, the vehicle will surface.

## IV. PNEUMATIC SYSTEM OVERVIEW

Regulating the volume ratio of water and air in ballast tanks controls buoyancy of the vehicle. The tanks have outlets at both ends so that water can flow in or out (Fig. 3). In the middle of the tank, there is an air expansion chamber made from rubber. When the chamber is filled with air, water will

drain from the tank and the buoyancy of the vehicle increases.

Both ends of the ballast tanks have also a place for trimming weights that can be used to compensate for the change of weight of the vehicle or adjust the centre of gravity when modules are changed or added.

The compressed air balloon supplies air at a pressure of approximately 8 at. This air is used to inflate the air expansion chambers in the ballast tanks. The compressed air balloon is connected to the chambers with air inlet hoses. A Y-branch divides the inlet path to two branches. There are two pairs of valves at both branches. The first pair of valves is outlet valves that can be controlled independently. This permits inflating or deflating only one of the air expansion chambers at time when the vehicle is operating in a laterally compressed configuration. The second pair of valves is the check valves that prevent water from intruding into the pneumatic system.

The air outlet hoses are attached between the air expansion chambers and openings at the frontal part of the vehicle. Like inlet paths, the outlet paths have check and outlet valves.

Both branches are connected together with additional Y-branches, a hose and an outlet valve near the frontal end of the pressured air balloon. This valve is opened when the vehicle is operating in a horizontally compressed configuration. This guarantees an equal pressure in both air expansion chambers and therefore improves pitch stability and controllability of the vehicle.

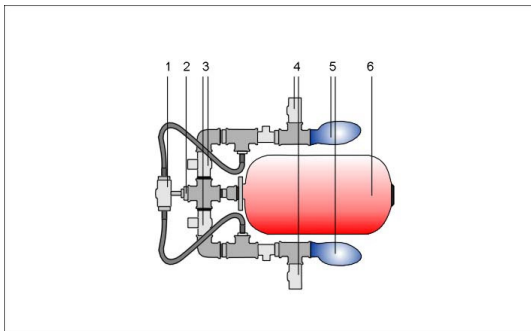


Fig. 3. Pneumatics

(1-pressure equalizing valve, 2-air inlet, 3-input valves, 4-output valves, 5-rubber tanks, 6-compressed air tank)

## V. CONTROL SYSTEM

Our robot has a three-layered control system as shown in Fig. 4. The upper layer is Texas Instrument's OMAP5912 Strong-ARM based microcomputer, which communicates with the offboard PC and is responsible for programming dive plan for the next layer. It also records and pre-processes video input.

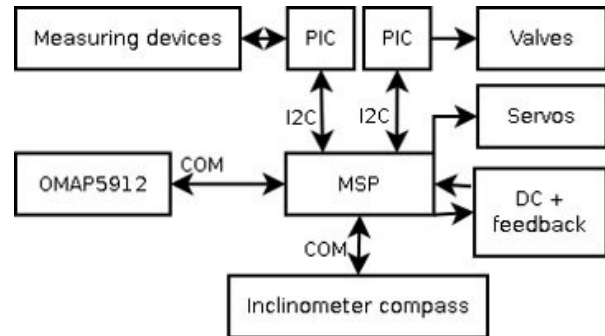


Fig. 4. Conceptual control system

The second layer is an ultra-low power 16-bit RISC mixed-signal processor Texas Instrument MSP430. It receives the dive plan from the upper layer Strong-Arm OMAP5912 via a serial port. The main task of this control layer is to follow the dive plan by controlling the actuators, and to collect inputs from sensors. Sensor input and performance of actuators is also recorded for later processing.

The third layer consists of an array of PIC processors that control the actuators and sensors. Some actuators have built-in PIC microprocessors while others (like valves) have external PIC processors. Communication between MSP430 and PIC processors is done via I2C protocol.

Active control of robot is done by MSP430, which is responsible for interpreting the dive plan, forwarding commands to lower level PIC controlled devices and communicating the results back to the upper layer OMAP5912. Since MSP430 has many PWM outputs, it is also directly driving the 2 servomotors and reading the tail position from the angle decoder connected to the DC motor of the tail.

The communication protocol is described in Fig. 5. Communication between the OMAP5912 and MSP430 layer is implemented by command language easily understandable by a human. Communication between MSP430 and PIC processors is implemented by binary transmission.

Human operator can program mission in a flexible way writing a program like: "turn left", "go forward", "give a temperature reading", etc

The second layer MSP430 converts this high level commands into a binary form for PIC processors, waits until the commands are executed and sends back the acknowledgement to the MSP430. This permits to save MSP430 processing time for other tasks like video signal recording and transmitting information back to the boat.

The OMAP5912 processor of the upper control layer can send 3 types of commands to the second layer MSP430: "insert sequence item", "start/stop sequence" and "device control". Syntax of the command is "*device identifier=command*". Each command is mirrored from MSP back to OMAP5912 to ensure the proper reception of the command.

Received commands are collected into the stack in the internal memory of MSP430 and are executed sequentially.

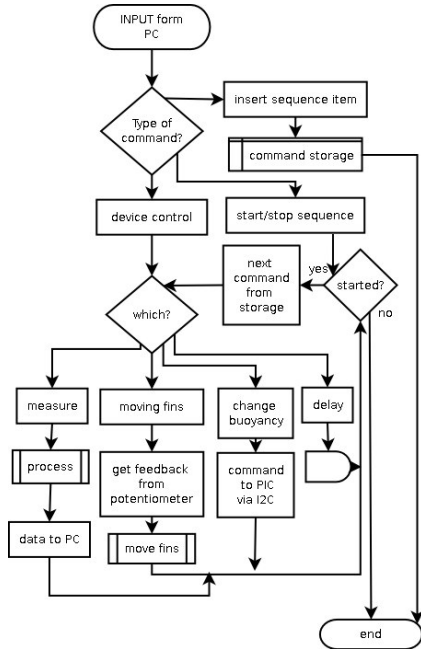


Fig. 5. Communication flow.

It is possible to start or stop processing sequence of commands by sending start/stop sequence instruction. It is also possible to control an individual device (e.g. a fin) by sending a single device control command.

## VI. EXPERIMENTAL SETUP

Preliminary experiments were conducted to test the functionality of the prototype of the robot and the feasibility of the design.

The first experiment was conducted outdoors in a pond to test the buoyancy control of the robot (Fig. 6). The second set of experiments was conducted in an indoor pool to evaluate the performance of the actuators (Fig. 7).

The goal of the pool tests was to measure the drag force of the robot's body and performance of the tail fin used as a steering device in the towing mode or a propulsion device in the autonomous mode

These experiments were done in a pool with the size 6,5m x 2,5 m. Water in the pool was 0.9m deep. The floor of the pool has colour stripes with the width of 0.24m. We used this pattern of the stripes to calculate the speed of the robot from the recorded videos.

To determine the drag force we towed the submerged robot with different speeds and measured the force at the same time.

To measure the performance of the tail the robot was powered by an external power supply. This allowed us to experiment with different supply voltages. A specially designed electronic circuit permits to change the PWM signal. The amplitude of the tail fin did not change.

We experimented with two different tail fin configurations, horizontal and vertical with respect to the body of the robot, while the robot's body was always in the horizontal configuration. The robot had zero buoyancy, so it was fully under water but did not touch the bottom. We also experimented with two different body weights. In the first

experiment the overall weight of the robot was 20 kg and in the second experiment we increased it up to 21,5 kg.

For tail fin movement we used a DC motor with a gearbox and an angle decoder. The motor driving the fin actuator was operating in 12V mode or in 17V mode.

The oscillating frequency of the tail movement frequency in 12 V modes is 0,26 Hz and in 17 V mode is 0,625 Hz, the amplitude of the tail is 0,8 m measured from the tip of the tail. , The area of the tail is 0,0866 cm<sup>2</sup>. Power consumption in the 17 V mode was 34W and in the 12V mode 18W.



Fig. 6. Pond test. Robot surfaces in vertical mode using only one side balloon.

## VII. TEST RESULTS

The goal of the pond experiment was to test the robot's ability to regulate buoyancy. The air tank was filled with air at 4 atm and 10 submerging tests were successfully done. The depth was 2 m. The robot submerged and surfaced both in horizontal and vertical modes as well as changed its orientation when the lower tank was inflated or deflated (Fig. 6).

The pool tests we conducted to measure the energy efficiency and speed of the self-propelled movement. We tried to find guidelines to develop optimal actuator movements, optimal points for attaching stabilizing fins, optimal body weight and optimal working regimes for the tail. The results of tests are in [15]. The drag force can be found from equation (1):

$$F_D = C_D \cdot \frac{1}{2} \cdot \rho \cdot v^2 \cdot S, \quad (1)$$

where  $C_D$  is the drag coefficient,  $\rho$  is the density of fluid,  $v$  is speed of the vehicle and  $S$  is the characteristic surface area of the robot.

We measured drag force and the speed of the vehicle (see Table I). Drag coefficient  $C_D$  can be estimated from equation

$$(2): C_D = \frac{2 \cdot F_D}{\rho \cdot v^2 \cdot S} \quad (2)$$

It depends on the chosen reference surface area  $S$ .



Fig 7. Pool test.

TABLE I.  
Drag test results and corresponding drag coefficients

speed $v$ (m/s)	Measured Drag force $F$ (N)	Drag coefficient 1	Drag coefficient 2
0.27	5	0.031	0.292
0.34	10	0.039	0.368
0.37	12	0.039	0.373

There are several different areas from which to choose when developing the reference area used in the drag equation. If we think of drag as being caused by friction between the water and the body, a logical choice would be the total surface area of the body. If we think of drag as being a resistance to the flow, a more logical choice would be the frontal area of the body which is perpendicular to the flow direction.

If we model the vehicle as an elliptical cylinder with the length  $L=1.45\text{m}$  and axes  $a=0.3\text{m}$  and  $b=0.5\text{m}$ , the total reference surface area for the drag coefficient calculation is

$$S = 2\pi ab + \pi(2 \cdot (a^2 + b^2))^{1/2} \cdot L = 4.44(\text{m}^2) \quad (3)$$

which is the total "wet surface" of the vehicle.

There is a slight difference between the drag coefficient of our vehicle compared with a cylindrical body with the similar ratio between the length and the diameter ( $L/D=4$ ). The drag coefficient of the cylindrical body is 0.048 [16].

The actual drag coefficient of our vehicle is smaller. The conclusion is that our robot is more streamlined than a cylinder with similar parameters. Approximation to cylinder with ratio  $L/D=7$  and with parallel flow ( $C_D=0.033$ ) could be used for modelling the robot.

We calculate drag coefficient 2 as cross section of elliptical cylinder with axes  $a=0.3\text{m}$  and  $b=0.5\text{m}$ . The total reference surface  $S$  would be

$$S = \pi ab = 0.47(\text{m}^2) \quad (4)$$

Compared to the ellipsoidal body in turbulent flow [17] the drag coefficient of our vehicle is about two to three times larger. The drag coefficient is about the same as of a cone with  $30^\circ$  angle.

The Reynolds number

$$\text{Re} = \frac{Lv}{\nu} \quad (5)$$

where  $L$  is characteristic length of the body,  $v$  is swimming speed and  $\nu$  is dynamic viscosity of water,  $\nu = 10^{-6} \frac{\text{m}^2}{\text{s}}$ . The Reynolds number is  $\text{Re} \approx 5 \cdot 10^5$

which could be interpreted as turbulent flow of water.

We conducted two sets of experiments to measure the performance of the tail fin. The results of the first set of experiments are presented in Table II.

The test results diverge a lot because robots body started to oscillate strongly. Oscillation decreases the speed and the robot even stopped some times. In tests 5-7 we disturbed the body oscillation using side fins.

TABLE II.  
Robot performance with 20 kg body weight in the first test

Time (s)	Speed (m/s)	Voltage (V)	Tail position	Tail movement	
1	373	0,017	12	vertical	Continuous
2	541	0,012	12	vertical	Continuous
3	193	0,033	12	vertical	Continuous
4	341	0,019	12	vertical	Continuous
5	150	0,043	12	vertical	Continuous
6	105	0,061	17	vertical	Continuous
7	96	0,067	17	horizontal	Continuous

TABLE III  
Robot performance with 21.5 kg weight in second test

Time (s)	Speed (m/s)	Voltage (V)	Tail position	Tail movement	
1	95	0,07	12	vertical	Continuous
2	155	0,04	12	vertical	Cyclic
3	60	0,11	17	vertical	Continuous
4	91	0,07	17	vertical	Cyclic
5	140	0,05	12	horizontal	Continuous
6	180	0,04	12	horizontal	Cyclic
7	73	0,09	17	horizontal	Continuous
8	90	0,07	17	horizontal	Cyclic
9	70	0,09	17	horizontal	Cyclic
10	90	0,07	17	horizontal	Cyclic
11	76	0,08	17	horizontal	Cyclic

In the second set of experiments represented in Table III we increased the robot's body weight up to 21,5 kg. This extra weight makes robot more stable and oscillation of the body almost ceases. We also experimented with two different frequencies and tail movement modes. In the continuous mode the tail worked periodically all the time. In the cyclic mode the tail executed two cycles, then rested in the middle position for 5 sec.

It can be seen that the test results depend on the body weight. When the robot weights less, the oscillation of the body decreases speed. Strong oscillation was also caused by too large amplitude of the tail fin and must be reduced in further tests. Observations of fish suggest that optimal tail turning angle is 10-20 degrees.

The tests also show that the orientation of the tail fin does not influence the performance of the robot. The horizontally attached fin did not have much advantage over the vertically attached fin. We can use this property to adjust or rotate the tail fin so that it creates less turbulence and does not decrease visibility.

The third conclusion is that it is possible to adjust tail movement cycles so that the robot does not lose speed. This means that we can preserve energy, because stopping tail movement for a while disturbs the oscillation of the body and therefore increases efficiency.

It is also possible to decelerate or even reverse the speed, if we can control tail movement and area.

We also measured the robot's ability to submerge using side fins if the robot was towed with approximate speed of 0,1 m/sec. The measured submerging speed was 0,025 m/sec.

## VIII. CONCLUSIONS AND FUTURE WORK

This paper describes the preliminary prototype of an underwater vehicle. The vehicle is built for environmental inspection in shallow waters of the Baltic Sea. The design concept is based on the environmental restrictions, human factors and cost requirements.

At present we have tested our robot in a pool and a pond. The test results show that the robot is functional but its efficiency can be increased. These preliminary test results can be used to redesign the robot. The goal for redesign is to achieve greater efficiency, speed and manoeuvrability. We are also developing the mathematical model that can predict our robot's performance, different tail sizes and shapes will be tested to find the optimal type of the tail. The field tests on the sea are scheduled for the coming ice-free season. In parallel we are developing control algorithms and computer vision software for automatic image processing to recognize different algae from the video input. We are developing also a small expert system for classification of seaweeds based on visual appearance, bottom and depth information. The result of this work gives knowledge about the vegetation to environmental scientists.

## IX. REFERENCES

- [1] E. Kim, Y. Youm, "Design and Dynamic Analysis of Fish Robot PoTuna." *Proceedings of the 2004 IEEE Int. Conf. on Robotics and Automation (ICRA 2004)*, New Orleans, LA, April 2004, pp. 4887-4892.
- [2] J.M.Anderson, M.S. Triantafyllou, P.A.Kerrebrock. "Concept Design of a Flexible-Hull Unmanned Undersea Vehicle." *Proceedings of the Int. Offshore and Polar Engineering Conf.*,1997, pp. 82-88.
- [3] D. McFarland, I. Gilhespy, E. Honary, "DIVEBOT: A Diving Robot with a Whale-like Buoyancy Mechanism." *Robotica*, Vol. 21, 2003, pp. 385 – 398.
- [4] M. Mojarrad, "AUV Biomimetic Propulsion," in *Proceedings of OCEANS 2000 MTS/IEEE Conference and Exhibition*, vol. 3 , 11-14 Sept. 2000, pp. 2141 – 2146
- [5] N. Kato, T. Inaba, "Guidance and Control of Fish Robot with Apparatus of Pectoral Fin Motion." *Proceedings. of the 2001 IEEE Int. Conf. on Robotics and Automation*, Leuven, Belgium, May 1998, pp. 446 – 451.
- [6] Y. Terada, I. Yamamoto. "An Animatronics System Including Lifelike Robotic Fish." *Proc. Of the IEEE*, Vol. 92. No. 11, November 2004, pp. 1814-1820.
- [7] J. Yu, M. Tan, S.Wang, E.Chen. „Development of a Biomimetic Robotic Fish and Its Control.“ *IEEE Trans. On Systems, Man and Cybernetics*, Vol. 34, No. 4, August 2004, pp. 1798-1810.
- [8] K. A. . McIsaac, J.P.Ostrowski, "Motion Planning for Anguilliform Locomotion." *IEEE Trans. On Robotics and Automation*, Vol. 19, No.4, August 2003, pp. 637 – 652.
- [2] G. Oliver, D. Avia, M. de Diego, A. Ortiz and J. Proenza. "RAO: A Low-Cost AUV for Testing." *OCEANS 2000 MTS/IEEE Conference and Exhibition*, 11-14 Sept. 2000, pp.397 – 401.
- [3] S. Williams, I. Mahon. "Simultaneous Localization and Mapping on the Great Barrier Reef." *Proceedings of the 2004 IEEE Int. Conf. on Robotics and Automation (ICRA 2004)*, New Orleans, LA, April 2004, pp. 1771-1776.
- [5] J.E.Colgate, K.M.Lynch, "Mechanics and Control of Swimming." *IEEE Jour. of Oceanic Engineering*, Vol.28. No. 3, July 2004, pp. 660-673.
- [9] M. Sfakiotakis, D.M. Lane, J.B.c. Davies, J.B.c. "An Experimental undulating-fin device using the parallel Bellows Actuator." *Proc. of the 2001 IEEE Int. Conf. on Robotics and Automation*, Seoul, Korea, May 21-25, 2001, pp. 2356-2362.
- [10] Andres Punning, Mart Anton, Maarja Kruusmaa, Alvo Aabloo, "A Biologically Inspired Ray-like Underwater Robot with Electroactive Polymer Pectoral Fins", *Proc. of the Int. IEEE Conf. Mechatronics and Robotics 2004 (MechRob'04)*, Vol. 2, pp. 241 - 245, 13. - 15. Sept. 2004, Aachen.
- [11] R.L. Wernli. "AUVs – A Technology Whose Time Has Come.", 2002. *Proceedings of the 2002 International Symposium on Underwater Technology*, 16-19 April 2002, pp. 309-314.
- [12] S. Liu, D.Wang, E.K.Poh, "A Nonlinear Observer For AUVs in Shallow Water Environment." *Proceedings of the 2004 IEEE/RJS Int. Conf. on Intelligent Robots and Systems (IROS 2004)*, Sept. 28 – Oct. 2, 2004, Sendai, Japan, pp. 1130-1135.
- [13] J.Yuh, "Design and Control of Autonomous Underwater Robots: A Survey." *Autonomous Robots*, Vol. 8, 2000, pp. 7-24.
- [14] R. Bachmayer, L. L. Whitcomb, and M. Grosenbaugh. "An accurate four-quadrant nonlinear dynamical model for marine thrusters: theory and experimental validation." *IEEE Journal of Oceanic Engineering*, 25(1) January 2000.
- [15] <http://tilda.vorguvara.ee/robot/>
- [16]Koichi Hirata and Syusuke Kawai, November 15, 2001 [http://www.nmri.go.jp/eng/khirata/fish/experiment/upf2001/body\\_e.html](http://www.nmri.go.jp/eng/khirata/fish/experiment/upf2001/body_e.html)
- [17] Fluid Mechanics with Student Resources CD-ROM, Frank White, McGraw-Hill Higher Education, ISBN : 0072831804